ACS Catalysis

Research Article

pubs.acs.org/acscatalysis

DFT Study on the Homogeneous Palladium-Catalyzed N-Alkylation of Amines with Alcohols

Guo-Ming Zhao,[†,‡] Hui-ling Liu,[*,†] Xu-ri Huang,[†] Xue Yang,[‡] and Yu-peng Xie[‡]

[†]Institute of Theoretical Chemistry, Jilin University, Changchun, 130023, China

[‡]College of Science, Jilin Institute of Chemical Technology, Jilin, 132022, China

Supporting Information

ABSTRACT: DFT methods and the energetic span model have been used to study the mechanism of the N-alkylation of amines with alcohols catalyzed by the $PdCl_2$/dppe/LiOH system (dppe = 1,2-bis(diphenylphosphino)ethane). The energetic results indicate that the most favorable pathway is the inner-sphere hydrogen transfer pathway, which consists of initiation of the three-coordinated active alkoxide complex $[Pd(PhCH_2O)(dppe)]^+$ (**Int4i**) and the catalytic cycle **CC1**. Initiation of **Int4i** includes two sequential steps: (i) generation of the three-coordinated active species $[Pd(OH)(dppe)]^+$ and $[Pd(PhNH)(dppe)]^+$ and (ii) $PhCH_2OH$ deprotonation with the aid of $[Pd(PhNH)(dppe)]^+$ to afford **Int4i**. Catalytic cycle **CC1** includes three sequential steps: (i) β-H elimination of **Int4i** to generate benzaldehyde and the Pd hydride species $[PdH(dppe)]^+$, (ii) condensation of benzaldehyde with aniline to give the imine, and (iii) imine reduction to supply the amine product and to regenerate **Int4i**. The calculated turnover frequencies (TOFs) support that **CC1** is the most favorable, although it is inhibited by the reverse process of $PhCH_2OH$ deprotonation catalyzed by $[Pd(PhNH)(dppe)]^+$. By calculating the degree of TOF control, we identify the TOF-determining intermediate (TDI) and the TOF-determining transition state (TDTS) in **CC1**, and find that all the influential intermediates are the off-cycle $LiCl_2^-$-coordinated complexes in the overall reaction pathway, which leads us to conclude that $LiCl_2^-$ is the TOF-affecting key species. Our additional calculations show that the TOF may be improved by the addition of AgOTf or $AgBF_4$, which can scavenge the Cl^- and supply the weak ligand OTf^- or BF_4^-. Hopefully, these results are useful for further catalyst development.

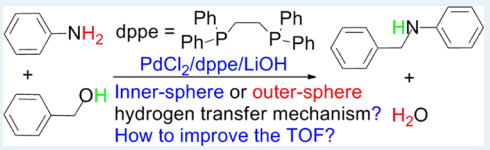

KEYWORDS: *DFT methods, the energetic span model, palladium catalyst, N-alkylation of amines, alcohols, hydrogen autotransfer mechanism*

INTRODUCTION

N-Alkyl amines play an important role in the syntheses of polymers, peptides, pharmaceuticals, and pesticides.[1] Hence, the development of efficient and environmentally benign methods for the synthesis of *N*-alkyl amines has been an important research area in organic chemistry.

As an attractive candidate for the synthesis of *N*-alkyl amines, the N-alkylation of amines with alcohols based on a so-called "hydrogen autotransfer"[2] or "borrowing hydrogen"[3] mechanism has attracted much attention in recent years. Compared with other *N*-alkyl methods of amines, e.g., the reaction of amines with alkyl halides,[4] the reductive amination reaction with carbonyl compounds,[5] hydroaminations,[6] and hydroaminomethylations,[7] this *N*-alkyl method has two obvious advantages: (1) alcohols are readily available, less toxic, and inexpensive; (2) theoretically, the only reaction byproduct is water. Since the first examples of the N-alkylation of amines with alcohols were reported in 1981,[8] this potentially green transformation has been extensively studied by experimentalists in the presence of the homogeneous transition metal complexes, such as Ru-,[9] Ir-,[10] Au-,[11] Ag-,[12] Rh-,[13] Cu-,[14] and Fe-based[15] complexes, and most of the experiments give good results.

The N-alkylation of amines with alcohols catalyzed by homogeneous transition metal complexes has also interested computational chemists. Their mechanistic investigations are mainly focused on Ru-[16,17] and Ir-catalyzed[18−21] alcohol oxidation and imine reduction: two key transformations for the N-alkylation of amines with alcohols. However, computational mechanistic studies on other metal complex-catalyzed N-alkylation of amines with alcohols are rare. To develop a simple and efficient catalytic system that can work under relatively mild conditions, mechanistic investigations on the N-alkylation of amines with alcohols catalyzed by other metal complexes are necessary.

Pd-based catalysts exhibited excellent catalytic activity in the N-alkylation of amines with allylic alcohols.[22] Attracted by the catalytic activity, Ramón and co-workers developed a $Pd(OAc)_2$ (1 mol %)/CsOH (100 mol %) catalyst system for the N-alkylation of amines with benzylic alcohols in 2011, giving up to 99% yield of the *N*-alkyl amines at temperatures of 130−150 °C with toluene as the solvent.[23] However, this catalytic system was reported to be not active under the optimized conditions when aliphatic or secondary alcohols were used as the alkylating agents. In 2013, a highly efficient and scalable homogeneous palladium catalytic system was developed by Seayad and co-workers for the N-alkylation of primary and cyclic secondary

Received: May 19, 2015
Revised: August 20, 2015
Published: August 24, 2015

DOI: 10.1021/acscatal.5b01043
ACS Catal. 2015, 5, 5728−5740

amines, and good to excellent yields (TON up to 900) were obtained when benzyl alcohol was used as the alkylating agent at 90−100 °C or when aliphatic and secondary alcohols were used as the alkylating agents at 130−150 °C.[24] On the basis of their experimental results and the similar Pd-catalyzed transformations,[25] Seayad and co-workers proposed a plausible catalytic cycle for the Pd-catalyzed N-alkylation of amines with alcohols. As shown in Scheme 1, the palladium alkoxide

Scheme 1. Seayad and Co-workers' Proposed Catalytic Cycle for the Pd-Catalyzed N-Alkylation of Amines with Alcohols[24]

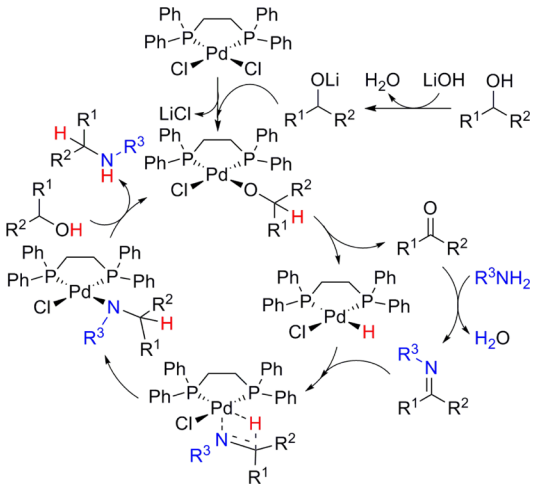

complex with a Cl^- ligand, $Pd(R^1R^2CHO)(dppe)Cl$, was postulated as the catalytically active species, which could generate the carbonyl compound $R^1R^2C{=}O$ and the Pd hydride PdH(dppe)Cl via β-H elimination. Then condensation of the carbonyl compound with the reactant amine R^3NH_2 supplied the imine $R^1R^2C{=}NR^3$ and water. The imine was successively reduced by the Pd hydride and R^1R^2CHOH via the sequential hydride and proton transfer processes to give the amine product and to regenerate the catalytically active species. Although the mechanism of the Pd-catalyzed N-alkylation of amines with alcohols has been proposed, the details of the transformation such as the feasibility of the four-coordinated Pd(II) complex $Pd(R^1R^2CHO)(dppe)Cl$ as the catalytically active species need to be scrutinized energetically. So far as we know, the mechanism of the Pd-catalyzed N-alkylation of amines with alcohols has not been studied in detail. Intrigued by the highly efficient and easily scaled-up characteristics of this new catalytic system, we perform a thorough DFT study to understand the catalytic mechanism. Our investigations show that all the active species are the cationic three-coordinated Pd(II) complexes without containing Cl^- ligands, and the Cl^- exists in the form of $LiCl_2^-$, which lowers down the TOF by coordinating to a three-coordinated complex to generate a more stable four-coordinated species.

COMPUTATIONAL DETAILS

All calculations were performed by using Gaussian 09 programs.[26] The fully optimized geometries of all species were obtained at the level of B3LYP[27,28] (SMD,[29] benzyl alcohol)/BSI, SMD corresponding to Truhlar and co-workers' solvation model which does an IEFPCM calculation with radii and nonelectrostatic terms, and BSI designating the basis set combination of LANL2DZ[30,31] for Pd and Ag and 6-31G(d,p)[32] for the other atoms. Harmonic frequencies were obtained at the same level of theory to characterize the stationary points as the minima (zero imaginary frequency) or transition states (one imaginary frequency) and to provide thermal corrections for Gibbs free energies and enthalpies at 373.15 K and 1 atm. Intrinsic reaction coordinate (IRC)[33] calculations were carried out to confirm that a transition state does connect two relevant minima. The single-point energies of the optimized geometries were calculated at the level of M06[34](SMD, benzyl alcohol)/BSII, BSII denoting the basis set combination of LANL2TZ(f)[31,35] for Pd and Ag and 6-311++G(2df,2p) for all the other atoms. Single-point energies corrected by the corresponding Gibbs free energy corrections were employed in the following discussions, unless otherwise specified. The enthalpy results, single-point energies corrected by enthalpy corrections, were also given out in the square brackets of figures for reference. Furthermore, M06/BSII//B3PW91[27,36]/BSI, M06/BSII//TPSSTPSS[37]/BSI, M06/BSII//PBE1PBE[38]/BSI, M06/BSII//M06/BSI, and wB97XD[39] /BSII//wB97XD/BSI calculations were also carried out on selective species to verify the dependence of the functional.

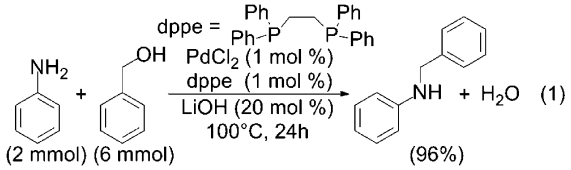

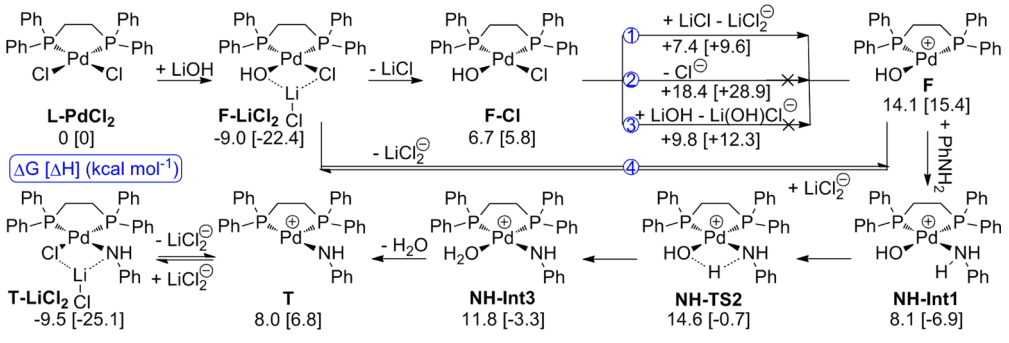

Figure 1. Generation of the three-coordinated active species **F** and **T**. The energies under the arrows (1, 2, 3) are the reaction energies.

DOI: 10.1021/acscatal.5b01043
ACS Catal. 2015, 5, 5728−5740

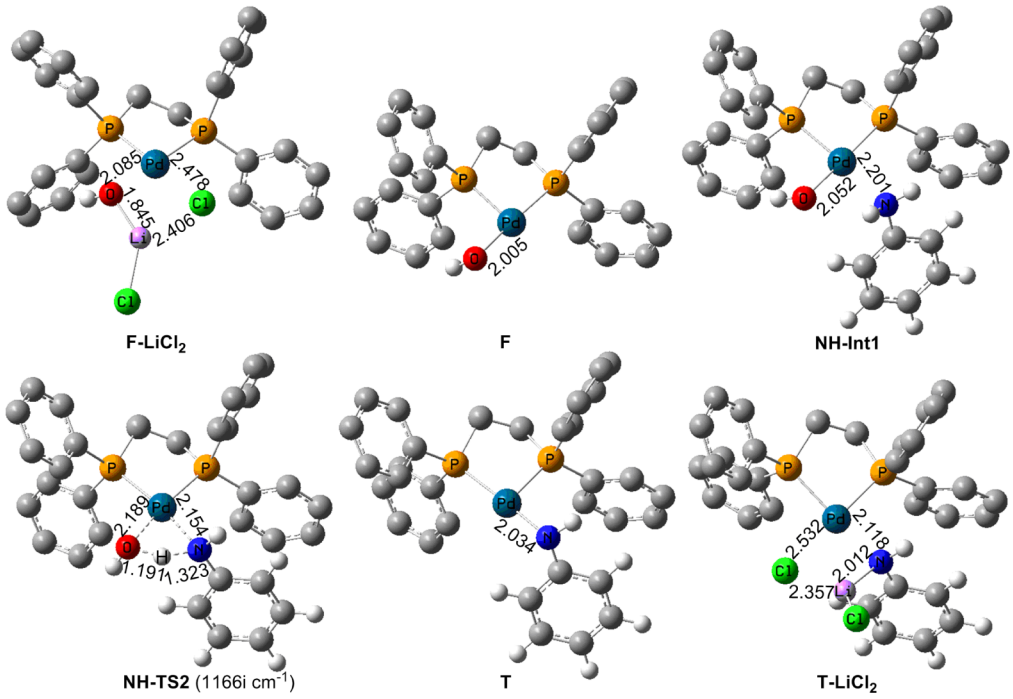

Figure 2. Optimized geometries of some key Pd(II) complexes shown in Figure 1. The important bond distances are given in Å, and the H atoms in the dppe ligand are omitted for clarity.

RESULTS AND DISCUSSION

Model Reaction. Molecular geometries and electronic structures of the substrates and catalyst have an important influence on the TOF of a catalytic reaction system, so in computational mechanistic studies, we prefer to employ the experimental substrates and catalyst rather than the simplified models.[18,40] In the present study, the experimental $PdCl_2$, dppe (1,2-bis(diphenylphosphino)ethane), and LiOH are employed as the catalyst, the ligand, and the base, respectively, and the N-alkylation of $PhNH_2$ with $PhCH_2OH$ is selected as the model reaction (eq 1).[24] Because $PhNH_2$ and $PhCH_2OH$ used in Seayad and co-workers' experiment are 2 and 6 mmol, respectively, $PhCH_2OH$ is treated as the solvent in the calculations.

Initiation of the Active Species. *Generation of the Three-Coordinated Active Species F and T.* At the beginning of the N-alkylation reaction of amines with alcohols, coordination of dppe to $PdCl_2$ gives the four-coordinated 16-electron Pd(II) d^8 complex **L-PdCl$_2$**. This coordination process is highly exergonic by 94.3 kcal mol^{-1}, so we choose **L-PdCl$_2$** as the energy reference point rather than $PdCl_2$ in the following discussions. Note that **L-PdCl$_2$** has no active site at the Pd center, so it is still a precatalyst. To obtain catalytically active species, the dissociation of the chloride ligands from the Pd(II) center is required. For this kind of dissociation, Noyori and co-workers have reported the base is necessary.[17] Therefore, we put **L-PdCl$_2$** and LiOH together to carry out the optimization calculation, and find that **L-PdCl$_2$** can easily react with LiOH to form the square-planar Pd(II) d^8 complex **F-LiCl$_2$**. As shown in Figure 1, in **F-LiCl$_2$**, one of the Cl^- ligands originally coordinating to the Pd center has been replaced by the OH^- ligand, and the dissociated Cl^- ligand coordinates to the Li center. The distances of Pd−O, Pd−Cl, Li···O, and Li···Cl in **F-LiCl$_2$** are 2.085, 2.478, 1.845, and 2.406 Å, respectively (Figure 2). However, **F-LiCl$_2$** is not yet an active species. For the generation of an active species from a four-coordinated square-planar d^8 organometallic complex, Hartwig has pointed out that the ligand dissociation can give the active species with a vacant coordination site.[41] Then, we consider the dissociation of the $LiCl_2^-$ ligand from **F-LiCl$_2$**, for it supplies a vacant coordination site at the Pd center and a proton acceptor site at the OH^- ligand. For the dissociation of $LiCl_2^-$, there are four possible pathways. The energetic results show that pathway 1 or 4 is the most favorable. In pathway 1, the release of LiCl from **F-LiCl$_2$** gives the four-coordinated Pd(II) chloride **F-Cl** with a free energy change of +15.7 kcal mol^{-1}. **F-Cl** with the aid of LiCl can produce the cationic three-coordinated 14-electron complex **F** at a free energy cost of 7.4 kcal mol^{-1}. In pathway 4, **F-LiCl$_2$** is directly ionized to the cation **F** and the anion $LiCl_2^-$ with a free energy change of +23.1 kcal mol^{-1}. However, we cannot conclude which pathway is more favorable on the basis of the present energetic results. We can only ascertain that the system existing in the form of **F** and $LiCl_2^-$ is the most favorable in the proposed ionization cases. The ionization processes in pathways 2 (**F-Cl** is directly ionized to **F** and Cl^-) and 3 (**F-Cl** with the aid of LiOH is ionized to **F** and $Li(OH)Cl^-$) are less favorable than those in pathways 1 and 4 by 11.0 and 2.4 kcal mol^{-1}, respectively, so pathways 2 and 3 are ruled out.

$PhNH_2$ is a competent ligand. After yielding the three-coordinated Pd(II) active species **F**, $PhNH_2$ can coordinate to it with a free energy change of −6.0 kcal mol^{-1}, leading to the formation of the intermediate **NH-Int1**. The transition state **NH-TS2** for the proton transfer (N···H = 1.323 Å and O···H = 1.191 Å) is located at a free energy of 6.5 kcal mol^{-1} above **NH-Int1**. This transition state connects to the H_2O-coordinated intermediate **NH-Int3**, which can afford the cationic three-coordinated 14-electron complex **T** by releasing a molecule of water. The Pd−N bonds in **NH-Int1**, **NH-TS2**, and **T** are 2.201, 2.154, and 2.034 Å, respectively, and the Pd−O bonds in **F**, **NH-Int1**, and **NH-TS2** are 2.005, 2.052, and 2.189 Å,

DOI: 10.1021/acscatal.5b01043
ACS Catal. 2015, 5, 5728−5740

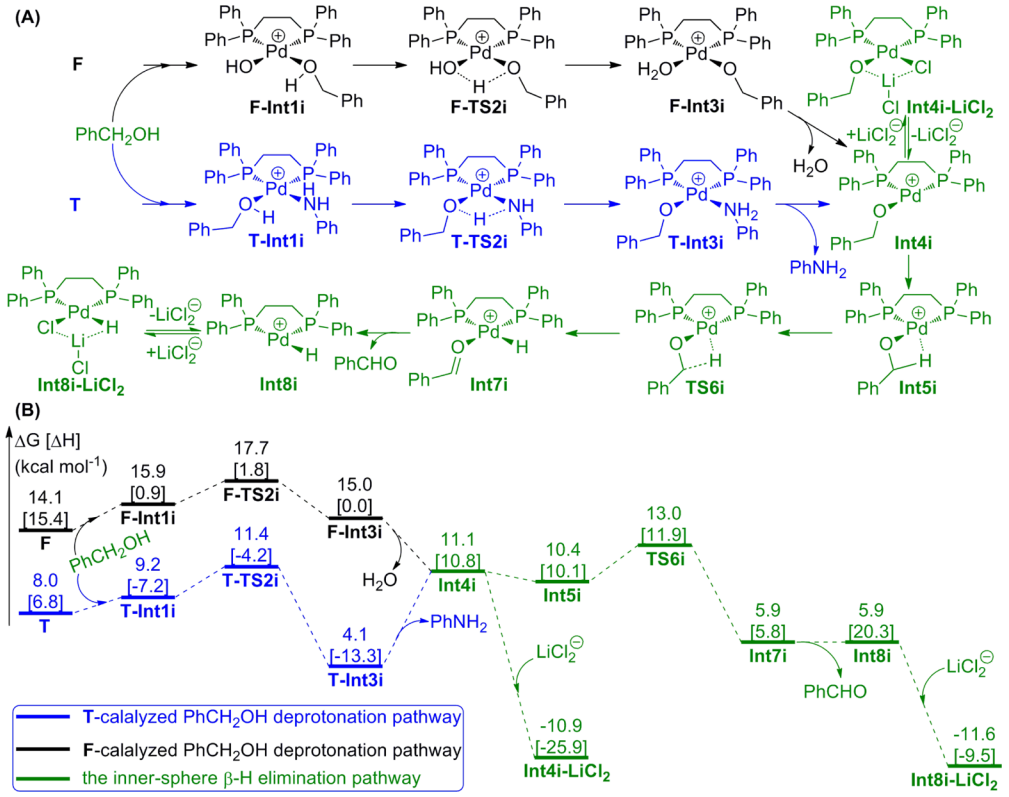

Figure 3. (A) Pathways for the initiation of the three-coordinated active alkoxide complex **Int4i** and for the formation of benzaldehyde and the Pd hydride species **Int8i**. (B) Free energy profiles corresponding to part A.

respectively, indicating that the Pd−N bond-forming process accompanies the Pd−O bond-breaking process.

Because the cationic complex **F** has a vacant coordination site at the Pd center, the counteranions in the reaction solution can easily coordinate to **F** to give the corresponding stable four-coordinated complexes. Comparing the $LiCl_2^-$-coordinated complex **F-LiCl$_2$** with the Cl^--coordinated complex **F-Cl**, OH^--coordinated complex **F−OH**, and $PhCH_2O^-$-coordinated complex **F-PhCH$_2$O**, we find that **F-LiCl$_2$** is the most stable (see eqs S1−S4 for the interactions of **F** with the possible counteranions). For the cationic three-coordinated complex **T**, we also consider that its fourth position is occupied by $LiCl_2^-$, Cl^-, OH^-, and $PhCH_2O^-$, and find that the $LiCl_2^-$-coordinated complex **T-LiCl$_2$** is the most stable (see eqs S5−S8 for the interactions of **T** with the possible counteranions). However, to ensure that the N-alkylation reaction continues, **F-LiCl$_2$** and **T-LiCl$_2$** have to release the $LiCl_2^-$ ligands to afford the corresponding three-coordinated active species. The dissociated free energies of $LiCl_2^-$ from **F-LiCl$_2$** and **T-LiCl$_2$** are 23.1 and 17.5 kcal mol^{-1}, respectively. Thus, **F-LiCl$_2$** and **T-LiCl$_2$** are considered as the off-cycle intermediates, which will supplant the corresponding three-coordinated complexes in the TOF calculations.[42] In the following discussions, the cationic three-coordinated 14-electron complexes **F** and **T** are postulated as the possible active catalysts for alcohol oxidation.

*Formation of the Three-Coordinated Active Alkoxide Complex **Int4i**.* The deprotonation of an alcohol to give the corresponding alkoxide complex is a vitally important transformation for the transition metal complex-catalyzed alcohol oxidation. Our previous studies have shown that the active catalyst with a deprotonated amine ligand can facilitate the deprotonation of an alcohol.[18] Thus, we first consider the **T**-catalyzed $PhCH_2OH$ deprotonation pathway. Coordination of $PhCH_2OH$ to **T** produces the well-prepared intermediate **T-Int1i** for the proton transfer (Figure 3A). This coordination process is favorable by 14.0 kcal mol^{-1} in terms of enthalpy, but slightly unfavorable by 1.2 kcal mol^{-1} in terms of free energy because of the entropy decrease (Figure 3B). Relative to **T-Int1i**, the transition state **T-TS2i** for the proton transfer has a free energy of 2.2 kcal mol^{-1}, in which the distances of O···H and N···H are 1.196 and 1.315 Å, respectively, confirming the O···H bond-breaking and N···H bond-forming processes (Figure 4). This transition state results in the $PhNH_2$-coordinated intermediate **T-Int3i**. By acquiring a free energy of 7.0 kcal mol^{-1}, **T-Int3i** can release the $PhNH_2$ ligand and afford the 14-electron alkoxide intermediate **Int4i** with an active site. The length of the Pd−O bond in **Int4i** is 2.012 Å, becoming shorter than that in **T-Int1i**, 2.274 Å, and in **T-TS2i**, 2.197 Å.

The **F**-catalyzed $PhCH_2OH$ deprotonation pathway is similar to the **T**-catalyzed $PhCH_2OH$ deprotonation process. Benzyl alcohol first coordinates to **F** at a free energy cost of 1.8 kcal mol^{-1}, giving the intermediate **F-Int1i**. Then the proton of benzyl alcohol transfers to the hydroxy ligand via the transition state **F-TS2i** ($PhCH_2O$···H = 1.220 Å and HO···H = 1.215 Å) with a free energy of 1.8 kcal mol^{-1} relative to **F-Int1i**, which results in the formation of the three-coordinated active alkoxide complex **Int4i** and water via the H_2O-coordinated intermediate **F-Int3i**.

Comparing the two pathways for the formation of the three-coordinated active alkoxide complex **Int4i**, we find that the overall **T**-catalyzed $PhCH_2OH$ deprotonation pathway (including the formation of the three-coordinated active species **T**) with an apparent activation energy of 23.6 kcal mol^{-1} (**NH-TS2**

DOI: 10.1021/acscatal.5b01043
ACS Catal. 2015, 5, 5728−5740

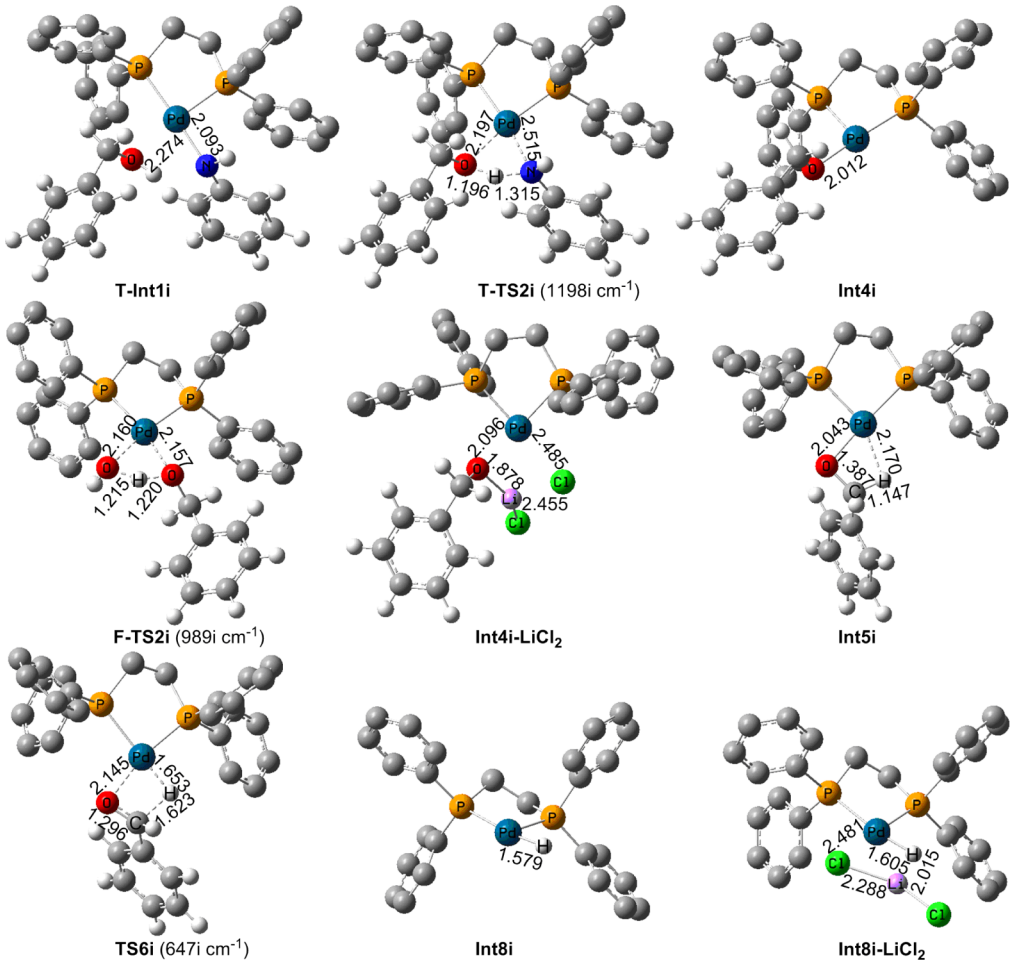

Figure 4. Optimized geometries of some key species shown in Figure 3. The important bond distances are given in Å, and the H atoms in the dppe ligand are omitted for clarity.

relative to (**F-LiCl$_2$** − $LiCl_2^-$ + $PhNH_2$)) is more favorable than the overall **F**-catalyzed $PhCH_2OH$ deprotonation pathway with an apparent activation energy of 26.7 kcal mol^{-1} (**F-TS2i** relative to (**F-LiCl$_2$** − $LiCl_2^-$ + $PhCH_2OH$)), consistent with our previous studies.[18,40]

Formation of Benzaldehyde and the Pd Hydride Species. *Inner-Sphere β-H Elimination Pathway.* Once the active alkoxide complex **Int4i** is produced, it will give benzaldehyde via an inner-sphere β-H elimination pathway. However, **Int4i** does not directly connect to the transition state **TS6i** for the β-H elimination (Figure 3). It must first isomerize to the agostic intermediate **Int5i**, in which the C−H and Pd···H distances are 1.147 and 2.170 Å, respectively (Figure 4). This agostic process is favorable by 0.7 kcal mol^{-1} in terms of both enthalpy and free energy. After many trials, however, we cannot find the transition state for the agostic step from **Int4i** to **Int5i**. Maybe this agostic step has a very late transition state, quite similar to **Int5i** in terms of both the geometry and free energy. Then the β-H elimination step from **Int5i** to **Int7i** takes place by passing the transition state **TS6i**, which has a four-membered geometry (C···H = 1.623 Å, Pd···H = 1.653 Å, and C−O = 1.296 Å), and which is only 2.6 kcal mol^{-1} higher than **Int5i**. This β-H elimination leads to the formation of the PhCHO-coordinated Pd hydride **Int7i**. Under the action of the favorable entropic driving force, the release of PhCHO from **Int7i** gives the 14-electron Pd hydride **Int8i** with a vacant coordination site.

Note that **Int4i** and **Int8i** each have a vacant coordination site at the Pd centers. Similar to **F** and **T**, $LiCl_2^-$ can coordinate to **Int4i** and **Int8i**, giving the off-cycle intermediates **Int4i-LiCl$_2$** and **Int8i-LiCl$_2$** (see eqs S9−S16 for the interactions of **Int4i** and **Int8i** with the possible counteranions). The dissociation of the $LiCl_2^-$ ligands from **Int4i-LiCl$_2$** and **Int8i-LiCl$_2$** to supply the corresponding three-coordinated active species requires Gibbs free energies of 22.0 and 17.5 kcal mol^{-1}, respectively.

The inner-sphere β-H elimination pathway proposed by Seayad and co-workers is also considered here. We first consider if Seayad and co-workers' proposed catalytically active alkoxide species Pd($PhCH_2O$)(dppe)Cl (**Int4i-Cl**) can directly afford benzaldehyde and the Pd hydride PdH(dppe)Cl (**Int8i-Cl**) via the β-H elimination (Scheme 1, when R^1 = Ph and R^2 = H). Because the Pd center of **Int4i-Cl** has no active site, we reason that the β-H elimination of **Int4i-Cl** cannot take place directly. The calculations confirm that there is no direct transition state for the β-H elimination of **Int4i-Cl**. Then we consider if the dissociation of one of the Pd−P bonds of **Int4i-Cl** can give the favorable transition state. However, the transition state **TS6i-Cl** (see Figure S1) for the β-H elimination is located at 41.6 kcal mol^{-1} above **Int4i-LiCl$_2$** − LiCl, which is too high to overcome in the experimental conditions (see eq 1). Thus, Seayad and co-workers' proposed catalytically active species can be ruled out. Because **Int4i-LiCl$_2$** is more stable than **Int4i-Cl**, we also consider the transition state **TS6i-LiCl$_2$**

DOI: 10.1021/acscatal.5b01043
ACS Catal. 2015, 5, 5728−5740

(see Figure S1) for the β-H elimination of **Int4i-LiCl$_2$**, which is as high as 35.5 kcal mol^{-1} relative to **Int4i-LiCl$_2$**. Therefore, this possibility is also ruled out.

Outer-Sphere Concerted Hydrogen Transfer Pathway. In this section, we will consider the **T**- and **F**-catalyzed outer-sphere concerted hydrogen transfer pathways for the generation of benzaldehyde. First, the **T**-catalyzed alcohol oxidation pathway is considered. As shown in Figures 5 and S2, the

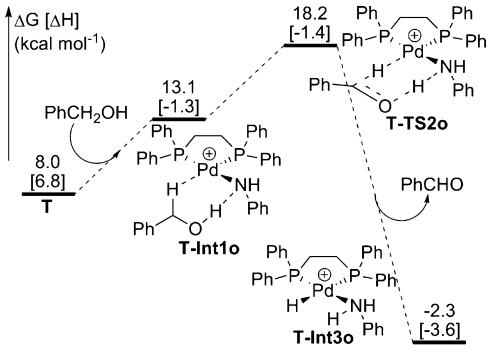

Figure 5. Free energy profile for the formation of benzaldehyde via the **T**-catalyzed outer-sphere concerted hydrogen transfer pathway.

binding of benzyl alcohol to **T** with an OH···N hydrogen bond of 1.834 Å and a CH···Pd bond of 2.641 Å affords the starting intermediate **T-Int1o** by requiring a free energy of 5.1 kcal mol^{-1}. The six-membered transition state **T-TS2o** for the concerted hydrogen transfer is located at a free energy of 5.1 kcal mol^{-1} above **T-Int1o**, in which the distances of O···H, N···H, C···H, and Pd···H are 1.309, 1.186, 1.216, and 1.879 Å, respectively. This transition state leads to the formation of PhCHO and the PhNH2-coordinated Pd hydride **T-Int3o**.

Second, we consider the **F**-catalyzed alcohol oxidation pathway. This pathway is similar to the **T**-catalyzed outer-sphere alcohol oxidation process. Benzyl alcohol first binds to **F** with a OH···O hydrogen bond of 1.695 Å and a CH···Pd bond of 2.645 Å by requiring a free energy of 8.3 kcal mol^{-1}, giving the initial intermediate **F-Int1o** (Figures 6 and S3). Then the

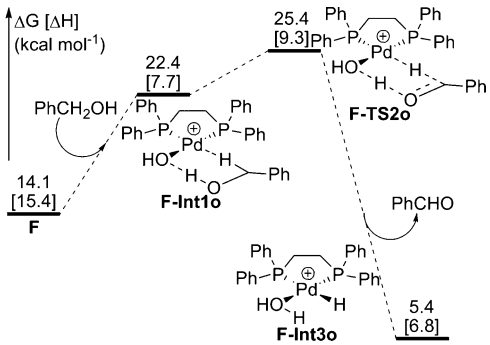

Figure 6. Free energy profile for the formation of benzaldehyde via the **F**-catalyzed outer-sphere concerted hydrogen transfer pathway.

hydroxy hydrogen and α hydrogen of benzyl alcohol transfer to the hydroxy ligand and the Pd center in a concerted manner via the six-membered transition state **F-TS2o** (PhCH$_2$O···H = 1.464 Å, HO···H = 1.308 Å, C···H = 1.400 Å, and Pd···H = 1.714 Å) with a free energy of 3.0 kcal mol^{-1} relative to **F-Int1o**, respectively, which results in the formation of PhCHO and the H$_2$O-coordinated Pd hydride **F-Int3o**.

In summary, we have discussed four possible pathways for the formation of benzaldehyde and the Pd hydride species in detail when considering the initiation of the active species. They are the inner-sphere β-H elimination pathway with the overall **T**-catalyzed PhCH$_2$OH deprotonation pathway, the inner-sphere β-H elimination pathway with the overall **F**-catalyzed PhCH$_2$OH deprotonation pathway, the overall **T**-catalyzed outer-sphere alcohol oxidation pathway (including the formation of the three-coordinated active species **T**), and the overall **F**-catalyzed outer-sphere alcohol oxidation pathway (including the formation of the three-coordinated active species **F**). The apparent activation energies in the above-mentioned four pathways are 23.9 (**TS6i** relative to (**Int4i-LiCl$_2$** − LiCl$_2^-$)), 26.7 (**F-TS2i** relative to (**F-LiCl$_2$** − LiCl$_2^-$ + PhCH$_2$OH)), 27.7 (**T-TS2o** relative to (**T-LiCl$_2$** − LiCl$_2^-$ + PhCH$_2$OH)), and 34.4 kcal mol^{-1} (**F-TS2o** relative to (**F-LiCl$_2$** − LiCl$_2^-$ + PhCH$_2$OH)), respectively. Thus, the most favorable pathway for the formation of benzaldehyde and the Pd hydride species is the inner-sphere β-H elimination pathway with the overall **T**-catalyzed PhCH$_2$OH deprotonation pathway. This most favorable benzaldehyde formation pathway is endergonic by 5.9 kcal mol^{-1}.

Imine Formation. The coupling of an aldehyde with an amine to produce an imine is a standard condensation reaction in organic chemistry. The mechanistic details of this condensation reaction depend on the reaction mixture. Hall and Smith's computational studies indicate that two concerted proton transfer processes of imine formation can be promoted by two water molecules.[43] Wang and co-workers found that an alcohol can also facilitate imine formation, and a water as the catalyst is more effective than an alcohol.[44] In our case, there are alcohols, aldehydes, amines, waters, and Pd(II) complexes in the reaction solution. Thus, the condensation reaction of benzaldehyde with aniline here may well be water-catalyzed, so we do not calculate the free energy profile for the imine formation, but only give the reaction free energy (PhCHO + PhNH$_2$ → PhCH═NPh + H$_2$O + 0.5 kcal mol^{-1}). This reaction free energy has been directly included in the initial point of the free energy profiles for the formation of the amine product in order to link with the free energy profiles for the formation of benzaldehyde and the Pd hydride species (see the next section).

Formation of the Amine Product and Regeneration of the Active Species. In this section, the three-coordinated Pd(II) hydride **Int8i** generated in the most favorable pathway for the formation of benzaldehyde and the imine PhCH═NPh formed in the aldehyde−amine condensation reaction are chosen as the initial reactants, and both the inner-sphere and the outer-sphere hydrogen transfer pathways are discussed in order to locate the most favorable pathway for the formation of the amine product and the regeneration of the active species.

Inner-Sphere Hydrogen Transfer Pathway. As shown in Figures 7 and 8, coordination of PhCH═NPh to **Int8i** produces the starting intermediate **Int9i**, which is more stable than **Int8i** + PhCH═NPh by 12.6 kcal mol^{-1}. The transition state **TS10i** for the hydride transfer is located at a free energy of 14.9 kcal mol^{-1} above **Int9i**, in which the distances of Pd···H and C···H are 1.643 and 1.617 Å, respectively. This four-membered transition state leads to the formation of the agostic intermediate **Int11i**, which has a similar geometry with **TS10i** (Pd···H = 1.960 Å and C−H = 1.166 Å). Although **Int11i** is 4.7 kcal mol^{-1} more stable than **TS10i**, the favorable driving forces of free energy, enthalpy, and entropy can promote the breaking

DOI: 10.1021/acscatal.5b01043
ACS Catal. 2015, 5, 5728−5740

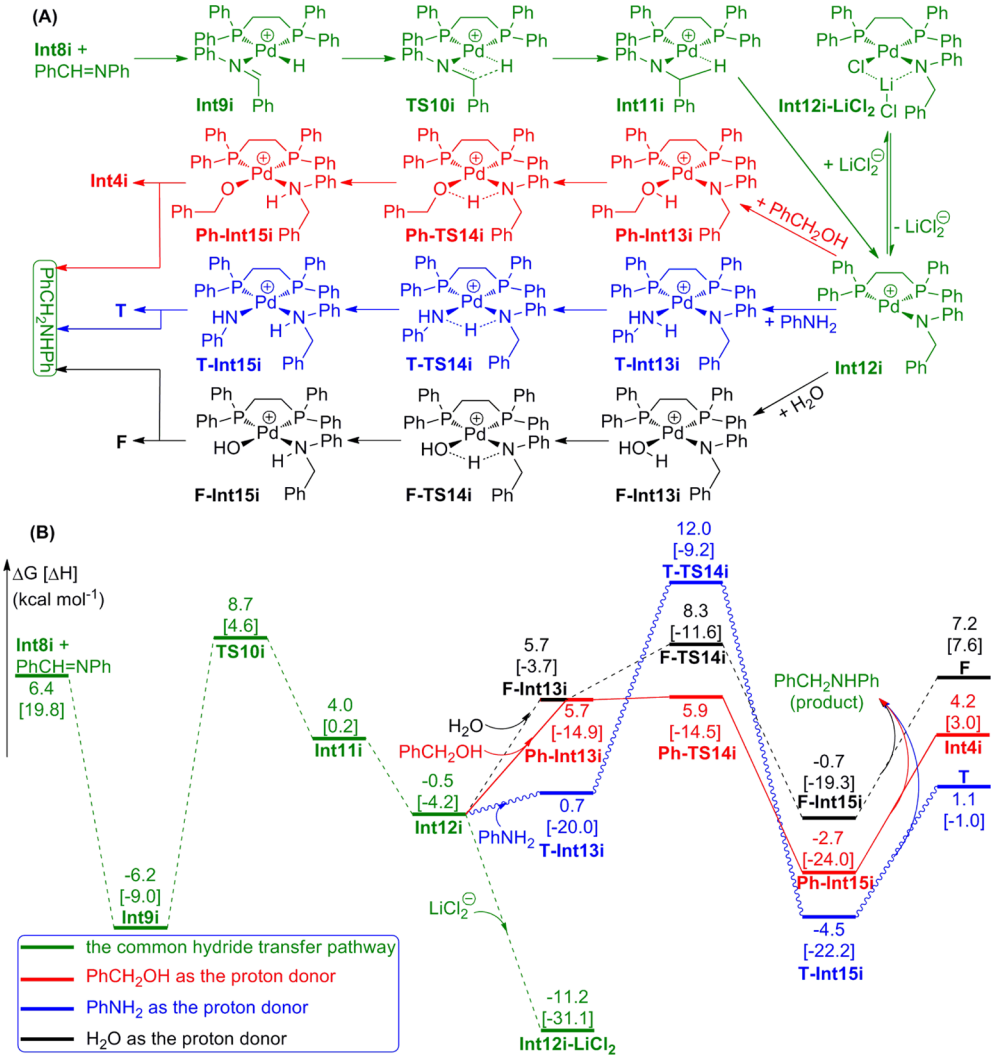

Figure 7. (A) Inner-sphere hydrogen transfer pathways for the formation of the amine product and the regeneration of the active species. (B) Free energy profiles corresponding to part A.

of the Pd···H bond to afford the 14-electron amido intermediate **Int12i** with a vacant coordination site, which is more stable than **Int11i** by 4.5 kcal mol^{-1}. After **Int12i** is obtained, $LiCl_2^-$ can coordinate to **Int12i** to yield the off-cycle intermediate **Int12i-LiCl$_2$**, from which the dissociation of the $LiCl_2^-$ ligand requires a free energy of 10.7 kcal mol^{-1} (see eqs S17−S20 for the interactions of **Int12i** with the possible counteranions).

Protonating the $PhCH_2NPh$ moiety of **Int12i** to deliver the amine product $PhCH_2NHPh$ has three possible pathways. In the case of $PhCH_2OH$ as the proton donor, coordination of $PhCH_2OH$ to **Int12i** generates the intermediate **Ph-Int13i** at a free energy cost of 6.2 kcal mol^{-1}. The transition state **Ph-TS14i** for the proton transfer is only 0.2 kcal mol^{-1} higher than **Ph-Int13i**, in which the O···H and N···H distances are 1.167 and 1.362 Å, respectively, confirming the O···H bond-dissociating and N···H bond-generating processes. This transition state leads to the formation of the amine product-coordinated alkoxide intermediate **Ph-Int15i**, which is more stable than the energy reference point by 2.7 kcal mol^{-1}. However, the favorable entropic force can promote the dissociation of the amine product from **Ph-Int15i**, resulting in the regeneration of the cationic three-coordinated Pd(II) active alkoxide complex **Int4i**. This dissociation process requires a free energy of 6.9 kcal mol^{-1}.

In the case of $PhNH_2$ as the proton donor, the starting $PhNH_2$-coordinated intermediate **T-Int13i** is 1.2 kcal mol^{-1} higher than $PhNH_2$ + **Int12i**. This intermediate can give the amine product-coordinated intermediate **T-Int15i** via the transition state **T-TS14i** with a relative free energy of 11.3 kcal mol^{-1} to **T-Int13i**. Intermediate **T-Int15i** is 4.5 kcal mol^{-1} more stable than the energy reference point, which can dissociate into the amine product and the cationic three-coordinated Pd(II) complex **T** by requiring a free energy of 5.6 kcal mol^{-1}.

In the case of H_2O as the proton donor, the proton transfer process is similar to that with $PhCH_2OH$ or $PhNH_2$ as the proton donor. H_2O first coordinates to **Int12i** at a free energy cost of 6.2 kcal mol^{-1}, delivering the intermediate **F-Int13i**. Then the proton transfer from the H_2O ligand to the $PhCH_2NPh$ moiety takes place via the transition state **F-TS14i** with a free energy of 2.6 kcal mol^{-1} relative to **F-Int13i**, yielding the amine product-coordinated intermediate **F-Int15i**. **F-Int15i** could further decompose into the amine product and the cationic three-coordinated Pd(II) complex **F** by costing a free energy of 7.9 kcal mol^{-1}.

DOI: 10.1021/acscatal.5b01043
ACS Catal. 2015, 5, 5728−5740

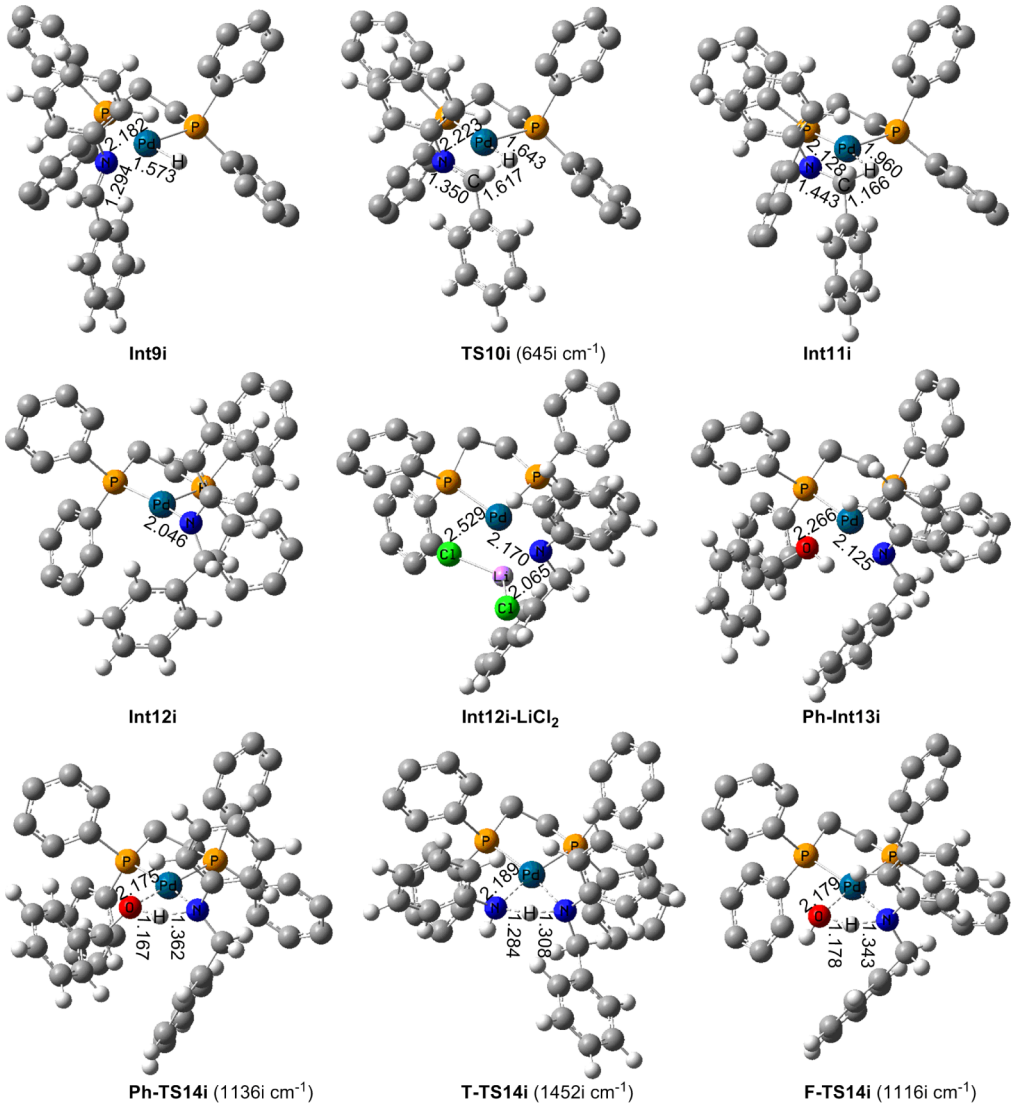

Figure 8. Optimized geometries of some key species shown in Figure 7. The important bond distances are given in Å, and the H atoms in the dppe ligand are omitted for clarity.

Seayad and co-workers' proposed inner-sphere imine reduction pathway with **Int8i-Cl** as the reduction species is considered here, and the inner-sphere imine reduction pathway with **Int8i-LiCl$_2$** as the reduction species is also considered because the off-cycle Pd hydride **Int8i-LiCl$_2$** is more stable than **Int8i-Cl** (see eqs S13 and S14). Since **Int8i-Cl** and **Int8i-LiCl$_2$** have no active sites at the Pd centers, the hydride transfer from **Int8i-Cl** or **Int8i-LiCl$_2$** to PhCH═NPh cannot take place directly. Then we consider if the dissociation of one of the Pd−P bonds of **Int8i-Cl** or **Int8i-LiCl$_2$** can give a favorable transition state. However, the calculation results show that the hydride transfer transition states **TS10i-Cl** and **TS10i-LiCl$_2$** are higher than the hydride transfer transition state **TS10i** by 17.1 and 10.9 kcal mol^{-1}, respectively (see Figure S4 for the schematic drawings of **TS10i-Cl** and **TS10i-LiCl$_2$**). Thus, the inner-sphere imine reduction pathway with **Int8i-Cl** or **Int8i-LiCl$_2$** as the reduction species is ruled out.

Outer-Sphere Concerted Hydrogen Transfer Pathway. The cationic complex **Int8i** has a vacant coordination site at the Pd center, so PhCH$_2$OH, PhNH$_2$, and H$_2$O each have an opportunity to coordinate to **Int8i**, generating the reduction species. After many attempts, however, the transition state for the imine reduction to give the amine product could be located only when the H$_2$O-coordinated complex **F-Int3o** was chosen as the reduction species. Thus, next we only discuss the outer-sphere imine reduction pathway with **F-Int3o** as the reduction species. As shown in Figures 9 and S5, the imine PhCH═NPh is bound to **F-Int3o** with a OH···N hydrogen bond of 1.704 Å to yield the starting intermediate **F-Int4o** by requiring a free energy of 7.6 kcal mol^{-1}. The transition state **F-TS5o** for the concerted hydrogen transfer has a six-membered structure, in which the distances of O···H, N···H, Pd···H, and C···H are 1.116, 1.415, 1.848, and 1.244 Å, respectively. Relative to **F-Int4o**, the free energy of **F-TS5o** is 11.2 kcal mol^{-1}. This transition state leads to the formation of the amine product and the regeneration of the cationic three-coordinated Pd(II) complex **F**.

In summary, we have discussed four possible pathways for the formation of the amine product and the regeneration of the active species in detail, which are the inner-sphere hydrogen transfer pathway with PhCH$_2$OH as the proton donor, the inner-sphere hydrogen transfer pathway with PhNH$_2$ as the proton donor, the inner-sphere hydrogen transfer pathway with H$_2$O as the proton donor, and the outer-sphere concerted

DOI: 10.1021/acscatal.5b01043
ACS Catal. 2015, 5, 5728−5740

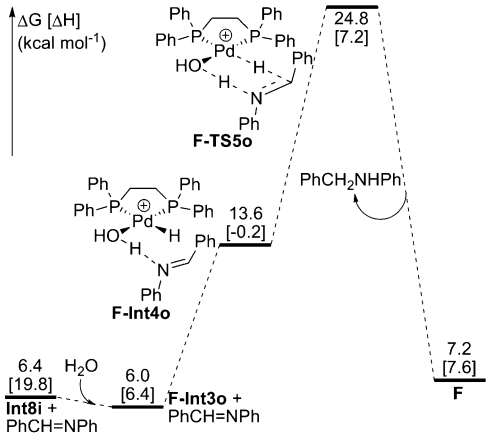

Figure 9. Free energy profile for the formation of the amine product via the outer-sphere concerted hydrogen transfer pathway with **F-Int3o** as the reduction species.

hydrogen transfer pathway with **F-Int3o** as the reduction species. The apparent activation energies in the above-mentioned four pathways are 20.3 (**TS10i** relative to (**Int8i-LiCl$_2$** − $LiCl_2^-$ + PhCH═NPh)), 23.6 (**T-TS14i** relative to (**Int8i-LiCl$_2$** − $LiCl_2^-$ + PhCH═NPh + $PhNH_2$)), 20.3 (**TS10i** relative to (**Int8i-LiCl$_2$** − $LiCl_2^-$ + PhCH═NPh)), and 36.4 kcal mol^{-1} (**F-TS5o** relative to (**Int8i-LiCl$_2$** − $LiCl_2^-$ + H_2O + PhCH═NPh)), respectively. These results only show that the first and the third pathways are more favorable than the second and the fourth pathways, but cannot tell which one is the most favorable. Therefore, we need to further compare the first and the third pathways. Figure 7B shows that the proton transfer barrier in the first pathway (17.1 kcal mol^{-1}, **Ph-TS14i** relative to (**Int12i-LiCl$_2$** − $LiCl_2^-$ + $PhCH_2OH$)) is lower than that in the third pathway (19.5 kcal mol^{-1}, **F-TS14i** relative to (**Int12i-LiCl$_2$** − $LiCl_2^-$ + H_2O)), so the most favorable pathway for the formation of the amine product and the regeneration of the active species is the inner-sphere hydrogen transfer pathway with $PhCH_2OH$ as the proton donor.

Discussion on the Overall Catalytic Transformation. Based on the above discussions, it can be found that the most favorable pathway for the formation of benzaldehyde and the Pd hydride species is initially the inner-sphere β-H elimination pathway with the overall **T**-catalyzed $PhCH_2OH$ deprotonation pathway and the most favorable pathway for the formation of the amine product and the regeneration of the active species is initially the inner-sphere hydrogen transfer pathway with $PhCH_2OH$ as the proton donor, and it can also be found that the most favorable pathway for the formation of the amine product regenerates the three-coordinated alkoxide complex **Int4i** rather than the initially postulated active catalyst **T** or **F** while affording the amine product. Thus, we conclude that the most favorable pathway for the Pd-catalyzed N-alkylation of amines with alcohols is the inner-sphere hydrogen transfer pathway, which is composed of initiation of the three-coordinated active alkoxide complex **Int4i** (Figure 1 and Figure 3A (blue pathway)) and the catalytic cycle **CC1** (Figure 3A (green pathway) and Figure 7A (green pathway + red pathway)). The reaction mechanism is illustrated in Scheme 2, formally similar to Seayad and co-workers' hypothesis (Scheme 1).

In our proposed mechanism, the cationic three-coordinated Pd(II) active species **F**, **T**, **Int4i**, **Int8i**, and **Int12i** all display 14-electron T-shaped structures. They are transient, but their chemical reactivity is vitally important for the N-alkylation reaction of amines with alcohols. Therefore, the stability and structural features of these complexes deserve closer attention. The free energies in Figures 1, 3B, and 7B indicate the following relative stability relation: **Int12i** > **Int8i** > **T** > **Int4i** > **F**. Because each three-coordinated complex has a dppe ligand and a vacant coordination site, their relative stability is determined only by their respective anionic ligands: $PhCH_2NPh^-$, H^-, $PhNH^-$, $PhCH_2O^-$, and OH^-. We first

Scheme 2. Mechanism for the Pd(II)-Catalyzed N-Alkylation of Aniline with Benzyl Alcohol

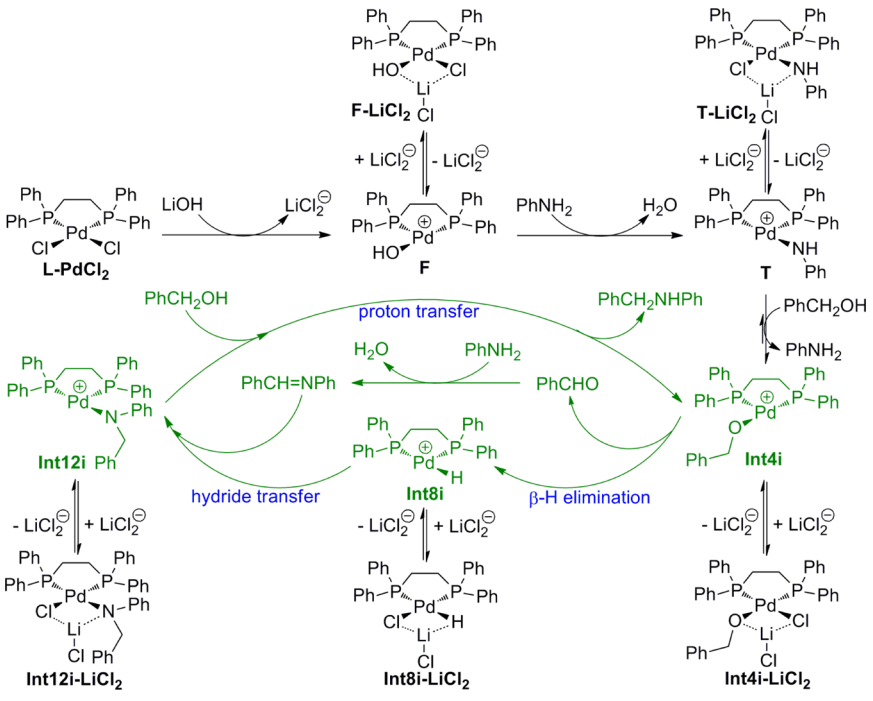

DOI: 10.1021/acscatal.5b01043
ACS Catal. 2015, 5, 5728−5740

Table 1. Key States, Free Energies (kcal mol^{-1}) at Different DFT Levels, TOF Values (h^{-1}), and Degree of TOF Control (in Brackets) for the Four Proposed Catalytic Cycles

key state	M06//B3LYP	M06//B3PW91	M06//TPSSTPSS	M06//PBE1PBE	M06//M06	wB97XD//wB97XD
Int4i-LiCl$_2$	−10.9 [0.99]	−12.1 [0.97]	−12.0 [0.99]	−13.5 [1.00]	−11.0 [0.73]	−16.2 [1.00]
TS6i	13.0 [0.99]	12.7 [0.97]	12.4 [0.98]	12.4 [1.00]	12.9 [0.75]	7.1 [0.99]
Int8i-LiCl$_2$	−11.6	−13.1	−12.2	−12.9	−13.8	−15.7
TS10i	8.7	9.0	8.7	6.5	8.6	3.2
Int12i-LiCl$_2$	−11.2	−12.9	−12.0	−12.3	−14.2	−18.0
Ph-TS14i	5.9	6.2	6.9	5.4	8.2	−4.9
TOF in **CC1**	277	79.2	140	19.1	205	612
T-LiCl$_2$	−9.5	−10.3	−10.4	−9.7	−12.4	−14.8
T-TS2i	11.4	12.3	13.3	11.6	13.3	4.5
T-TS14i	12.0	10.3	11.7	10.6	13.1	1.3
TOF in **CC2**	112	57.6	50.4	16.6	1.51	540
F-LiCl$_2$	−9.0	−10.1	−7.8	−9.9	−11.3	−14.6
NH-TS2	14.6	13.9	15.6	15.68	15.8	8.4
F-TS14i	8.3	7.9	7.9	8.7	7.4	0.6
TOF in **CC3**	144	50.4	79.2	11.2	2.84	324
F-TS2i	17.7	16.8	17.1	15.72	17.2	10.3
TOF in **CC4**	6.12	4.68	43.2	10.8	0.576	64.8

consider the electronic effects of these anionic ligands. The electron donating ability of these anionic ligands can be obtained from the natural bond orbital (NBO) calculations.[45] The NBO charges on the Pd atoms in **Int12i**, **Int8i**, **T**, **Int4i**, and **F** are 0.144, 0.118, 0.188, 0.325, and 0.320 e, respectively, which indicates that the order of the electron donating ability of the anionic ligands is H^- > $PhCH_2NPh^-$ > $PhNH^-$ > OH^- > $PhCH_2O^-$. This order is not completely inconsistent with the above relative stability order. The order of the electron donating ability, H^- > $PhNH^-$, $PhCH_2NPh^-$ > $PhNH^-$, $PhNH^-$ > OH^-, and $PhNH^-$ > $PhCH_2O^-$, is consistent with the above relative stability order. Then, we consider the steric effects of these anionic ligands. Note that $PhCH_2NPh^-$ and $PhCH_2O^-$ are much bulkier than H^- and OH^-, respectively, while the NBO charges on the Pd atoms in **Int12i** and **Int4i** are only marginally more than those in **Int8i** and **F**, respectively, so **Int12i** and **Int4i** are more stable than **Int8i** and **F**, respectively. Thus, the relative stability of these cationic three-coordinated Pd(II) complexes is determined by both electronic effects and steric effects of the anionic ligands, consistent with Lledós and co-workers' conclusion.[46]

The three-coordinated active species found here are similar to Martín-Matute and co-workers' proposed active complex **INT-1**:[47] they are all cationic complexes with a vacant coordination site at their respective metal centers, but different from our recently proposed active catalyst **C**,[18] a neutral complex with a vacant coordination site at the Ir center. One of the important reasons for the formation of the active cationic complex in Martín-Matute and co-workers' proposed mechanism is that BF_4^- is a weakly coordinating counteranion. However, in our present study, $LiCl_2^-$ is not a weakly coordinating counteranion. The dissociation of $LiCl_2^-$ from **F-LiCl$_2$** requires a free energy of 23.1 kcal mol^{-1}, the highest free energy required by the dissociation of $LiCl_2^-$ from the $LiCl_2^-$-coordinated complexes (see Figures 1, 3B, and 7B). But the apparent activation energy for the overall most favorable pathway is only 23.9 kcal mol^{-1} (Figure 3B, **TS6i** relative to (**Int4i-LiCl$_2$** − $LiCl_2^-$)), so these cationic three-coordinated Pd(II) active complexes are accessible.

Note that the transition state **TS6i** in the inner-sphere β-H elimination pathway of catalytic cycle **CC1** is 1.6 kcal mol^{-1} higher than **T-TS2i** in the **T**-catalyzed $PhCH_2OH$ deprotonation pathway, so the reverse process of the **T**-catalyzed $PhCH_2OH$ deprotonation pathway, from **Int4i-LiCl$_2$** (supplanting **Int4i**) to **T-LiCl$_2$** (supplanting **T**), can inhibit the TOF of **CC1**. However, the inhibition is thermodynamically unfavorable, and for this microscopic reversible reaction, the excess benzyl alcohols (see eq 1) can promote the forward reaction,[48] i.e., facilitate the **Int4i**-yielding reaction, so there will be little inhibition effect. In the following TOF calculations, this inhibition will be omitted. Also note that the transition state **TS6i** is 1.6 kcal mol^{-1} lower than **NH-TS2i** in the formation of **T**, and 4.7 kcal mol^{-1} lower than **F-TS2i** in the **F**-catalyzed $PhCH_2OH$ deprotonation pathway. Therefore, the reverse processes of the formation of **T** and of the **F**-catalyzed $PhCH_2OH$ deprotonation pathway have no effect on the TOF of **CC1**.

To further confirm that **CC1** is the most favorable catalytic cycle, a Fortran program[49] developed for the energetic span model[50] (see the Supporting Information for the energetic span model) is employed to calculate the TOFs of the four proposed lower-energy catalytic cycles (**CC1**, **CC2** (Figure 3A (blue pathway + green pathway) and Figure 7A (green pathway + blue pathway)), **CC3** (Figure 1, Figure 3A (blue pathway + green pathway), and Figure 7A (green pathway + black pathway)), and **CC4** (Figure 3A (black pathway + green pathway) and Figure 7A (green pathway + black pathway))). With this program, we also calculate the degree of TOF control (X_i) to identify the influential species on the TOFs. To test the functional dependence, we recalculate the free energies of the key states. All the calculated results are selectively collected in Table 1. On the basis of the first two columns of Table 1, we draw the following conclusions: (1) **CC1** possesses the highest TOF, 277 h^{-1}, which confirms that **CC1** is the most favorable catalytic cycle. (2) The TDI and TDTS in **CC1** are the $LiCl_2^-$-coordinated alkoxide complex **Int4i-LiCl$_2$** with $X_{TOF,I}$ = 0.99 and the transition state **TS6i** for the β-H elimination with $X_{TOF,T}$ = 0.99, respectively. (3) The important difference between **CC3** and **CC4** is the $PhCH_2OH$ deprotonation processes. This difference causes the TOF of **CC3** to be much higher than that of **CC4**, which indicates that the $PhCH_2OH$ deprotonation process catalyzed by **T** is more favorable than

DOI: 10.1021/acscatal.5b01043
ACS Catal. 2015, 5, 5728−5740

that catalyzed by **F**. This conclusion can be attributed to the fact that **T** is more stable than **F** because the barrier for the $PhCH_2OH$ deprotonation with **T** is only marginally higher than with **F** (Figure 3B). (4) All the influential intermediates are the off-cycle $LiCl_2^-$-coordinated complexes, such as **F-LiCl$_2$**, **T-LiCl$_2$**, **Int4i-LiCl$_2$**, **Int8i-LiCl$_2$**, and **Int12i-LiCl$_2$**. Thus, $LiCl_2^-$ is the TOF-affecting key species. Then, we consider whether the addition of AgOTf or $AgBF_4$ can improve the TOF. Equations S21−S32 show that the addition of AgOTf or $AgBF_4$ can scavenge chloride anion and offer weakly coordinating counteranion OTf^- or BF_4^-. With these new findings, we reassess the catalytic cycle **CC1** using the energetic span model. We find that OTf- or BF_4-coordinated complexes are no longer the influential intermediates, and the TOF of **CC1** after the addition of AgOTf or $AgBF_4$ is about 10^6 times faster than that in the model reaction. These findings may be useful for further catalyst development. (5) When calculating the TOF of **CC1**, we omit the inhibition of the reverse process of the **T**-catalyzed $PhCH_2OH$ deprotonation pathway. When the inhibition on **CC1** is considered, the major difference between **CC1** and catalytic cycles **CC2** and **CC3** is the different proton transfer processes in the formation of the amine product. However, Figure 7B shows that $PhCH_2OH$ is the most favorable among the three proton donors. Thus, even if the inhibition of the reverse process of the **T**-catalyzed $PhCH_2OH$ deprotonation pathway is considered, the catalytic cycle **CC1** is still the most favorable. The calculation results at different DFT levels consistently support the above conclusions.

Moreover, to further verify the mechanism obtained at the M06//B3LYP level, we also consider the basis set superposition error (BSSE) corrections with the counterpoise method[S1] and the entropic corrections by artificially raising the pressure[S2] for the key species. From the calculated results, shown in Table S1, we find that the most favorable pathway (including initiation of the three-coordinated active alkoxide complex **Int4i** and the catalytic cycle **CC1**) with the BSSE corrections or entropic corrections is consistent with that without these two corrections. Thus, the proposed mechanism shown in Scheme 2 is reliable for the title reaction.

CONCLUSIONS

This DFT study may provide important insights for understanding the N-alkylation of amines with alcohols catalyzed by the $PdCl_2$/dppe/LiOH system. The most favorable reaction pathway found here (Scheme 2) consists of initiation of the three-coordinated active alkoxide complex **Int4i** and the catalytic cycle **CC1**, which is formally similar to Seayad and co-workers' hypothesis (Scheme 1), but different in most of the details. In our proposed inner-sphere hydrogen transfer pathway, the generation of the active alkoxide complex **Int4i** does not need the formation of the lithium alkoxide. Instead, it requires that the palladium precursor **L-PdCl$_2$** with the aid of LiOH first yields the three-coordinated active species **F**, and then **F** reacts with the reactant $PhNH_2$ to afford the three-coordinated active species **T**. After $PhCH_2OH$ is deprotonated by **T**, **Int4i** is obtained and the reaction enters the catalytic cycle **CC1**. Catalytic cycle **CC1** is composed of β-H elimination of **Int4i** to generate benzaldehyde and the Pd hydride species **Int8i**, imine formation, and imine reduction to supply the amine product $PhCH_2NHPh$ and to regenerate the active alkoxide complex **Int4i**. The calculation results indicate that all the active species in the overall catalytic transformation do not include Cl^- ligands. The Cl^- exits in the form of $LiCl_2^-$, which can coordinate to a cationic three-coordinated complex to form an off-cycle intermediate. Thus, $LiCl_2^-$ is the TOF-affecting key species. Our additional calculations show that the TOF may be improved by the addition of AgOTf or $AgBF_4$, which can scavenge the Cl^- and supply the weak ligand OTf^- or BF_4^-. Hopefully, this mechanistic study will be helpful for further development of more efficient Pd catalysts.

ASSOCIATED CONTENT

Supporting Information

The Supporting Information is available free of charge on the ACS Publications website at DOI: 10.1021/acscatal.5b01043.

Equations; schematic drawings; optimized geometries; the energetic span model; Fortran program for TOF and X_i calculations; Cartesian coordinates, energies, and thermal corrections to enthalpies and free energies (PDF)

AUTHOR INFORMATION

Corresponding Author

*E-mail: huiling@jlu.edu.cn.

Notes

The authors declare no competing financial interest.

ACKNOWLEDGMENTS

The authors thank the National Basic Research Program of China (973 Program; 2012CB932800), the National Natural Science Foundation of China (No. 21303067, No. 21373099, No. 11447194), Doctoral Fund of Ministry of Education of China (No. 20130061110020), and Scientific Research Fund of Jilin Provincial Education Department (2015437) for financial support of this research. The authors also thank Mathematics Experiment Center, Jilin Institute of Chemical Technology, for computer support.

REFERENCES

(1) (a) *Amino Group Chemistry: From Synthesis to the Life Sciences*; Ricci, A., Ed.; Wiley-VCH: Weinheim, 2008; pp 207. (b) Lawrence, S. A. *Amines: Synthesis, Properties, and Applications*; Cambridge University: Cambridge, 2004; pp 265−305.

(2) Guillena, G.; Ramón, D. J.; Yus, M. *Angew. Chem., Int. Ed.* **2007**, *46*, 2358−2364.

(3) Edwards, M. G.; Jazzar, R. F.; Paine, B. M.; Shermer, D. J.; Whittlesey, M. K.; Williams, J. M. J.; Edney, D. D. *Chem. Commun.* **2004**, 90−91.

(4) (a) Singh, C. B.; Kavala, V.; Samal, A. K.; Patel, B. K. *Eur. J. Org. Chem.* **2007**, *2007*, 1369−1377;(b) Romera, J. L.; Cid, J. M.; Trabanco, A. A. *Tetrahedron Lett.* **2004**, *45*, 8797−8800;(c) Chiappe, C.; Pieraccini, D. *Green Chem.* **2003**, *5*, 193−197;(d) Salvatore, R. N.; Nagle, A. S.; Jung, K. W. *J. Org. Chem.* **2002**, *67*, 674−683.

(5) (a) Storer, R. I.; Carrera, D. E.; Ni, Y.; MacMillan, D. W. C. *J. Am. Chem. Soc.* **2006**, *128*, 84−86;(b) Mizuta, T.; Sakaguchi, S.; Ishii, Y. *J. Org. Chem.* **2005**, *70*, 2195−2199;(c) Abdel-Magid, A. F.; Carson, K. G.; Harris, B. D.; Maryanoff, C. A.; Shah, R. D. *J. Org. Chem.* **1996**, *61*, 3849−3862;(d) Bhattacharyya, S. *J. Org. Chem.* **1995**, *60*, 4928−4929.

(6) (a) Pan, S. G.; Endo, K.; Shibata, T. *Org. Lett.* **2012**, *14*, 780−783;(b) Werkmeister, S.; Fleischer, S.; Zhou, S. L.; Junge, K.; Beller, M. *ChemSusChem* **2012**, *5*, 777−782;(c) Mukherjee, A.; Nembenna, S.; Sen, T. K.; Sarish, S. P.; Ghorai, P. K.; Ott, H.; Stalke, D.; Mandal, S. K.; Roesky, H. W. *Angew. Chem., Int. Ed.* **2011**, *50*, 3968−3972; (d) Reznichenko, A. L.; Nguyen, H. N.; Hultzsch, K. C. *Angew. Chem., Int. Ed.* **2010**, *49*, 8984−8987.

DOI: 10.1021/acscatal.5b01043
ACS Catal. 2015, 5, 5728−5740

(7) (a) Müller, T. E.; Hultzsch, K. C.; Yus, M.; Foubelo, F.; Tada, M. *Chem. Rev.* **2008**, *108*, 3795−3892;(b) Ahmed, M.; Bronger, R. P. J.; Jackstell, R.; Kamer, P. C. L.; van Leeuwen, P. W. N. M.; Beller, M. *Chem. - Eur. J.* **2006**, *12*, 8979−8988;(c) Zimmermann, B.; Herwig, J.; Beller, M. *Angew. Chem., Int. Ed.* **1999**, *38*, 2372−2375.
(8) (a) Grigg, R.; Mitchell, T. R. B.; Sutthivaiyakit, S.; Tongpenyai, N. *J. Chem. Soc., Chem. Commun.* **1981**, 611−612;(b) Watanabe, Y.; Tsuji, Y.; Ohsugi, Y. *Tetrahedron Lett.* **1981**, *22*, 2667−2670.
(9) (a) Weickmann, D.; Frey, W.; Plietker, B. *Chem. - Eur. J.* **2013**, *19*, 2741−2748;(b) Cui, X.; Deng, Y.; Shi, F. *ACS Catal.* **2013**, *3*, 808−811;(c) Fernandez, F. E.; Puerta, C.; Valerga, P. *Organometallics* **2012**, *31*, 6868−6879;(d) Kawahara, R.; Fujita, K.; Yamaguchi, R. *Adv. Synth. Catal.* **2011**, *353*, 1161−1168;(e) Kawahara, R.; Fujita, K.-I.; Yamaguchi, R. J. *J. Am. Chem. Soc.* **2010**, *132*, 15108−15111.
(10) (a) Wetzel, A.; Wöckel, S.; Schelwies, M.; Brinks, M. K.; Rominger, F.; Hofmann, P.; Limbach, M. *Org. Lett.* **2013**, *15*, 266−269;(b) Wang, D.; Guo, X.-Q.; Wang, C.-X.; Wang, Y.-N.; Zhong, R.; Zhu, X.-H.; Cai, L.-H.; Gao, Z.-W.; Hou, X.-F. *Adv. Synth. Catal.* **2013**, *355*, 1117−1125;(c) Bartoszewicz, A.; Marcos, R.; Sahoo, S.; Inge, A. K.; Zou, X.; Martin-Matute, B. *Chem. - Eur. J.* **2012**, *18*, 14510−14519; (d) Cumpstey, I.; Agrawal, S.; Borbas, K. E.; Martin-Matute, B. *Chem. Commun.* **2011**, *47*, 7827−7829;(e) Michlik, S.; Kempe, R. *Chem. - Eur. J.* **2010**, *16*, 13193−13198.
(11) (a) He, L.; Qian, Y.; Ding, R.-S.; Liu, Y.-M.; He, H.-Y.; Fan, K.-N.; Cao, Y. *ChemSusChem* **2012**, *5*, 621−624;(b) Zotova, N.; Roberts, F. J.; Kelsall, G. H.; Jessiman, A. S.; Hellgardt, K.; Hii, K. K. M. *Green Chem.* **2012**, *14*, 226−232;(c) Tang, C.-H.; He, L.; Liu, Y.-M.; Cao, Y.; He, H.-Y.; Fan, K.-N. *Chem. - Eur. J.* **2011**, *17*, 7172−7177;(d) He, L.; Lou, X. B.; Ni, J.; Liu, Y. M.; Cao, Y.; He, H. Y.; Fan, K. N. *Chem. - Eur. J.* **2010**, *16*, 13965−13969.
(12) (a) Shimizu, K.; Shimura, K.; Nishimura, M.; Satsuma, A. *RSC Adv.* **2011**, *1*, 1310−1317;(b) Cui, X.; Zhang, Y.; Shi, F.; Deng, Y. *Chem. - Eur. J.* **2011**, *17*, 1021−1028.
(13) Satyanarayana, P.; Reddy, G. M.; Maheswaran, H.; Kantam, M. L. *Adv. Synth. Catal.* **2013**, *355*, 1859−1867.
(14) (a) Dixit, M.; Mishra, M.; Joshi, P. A.; Shah, D. O. *Catal. Commun.* **2013**, *33*, 80−83;(b) Martínez-Asencio, A.; Ramón, D. J.; Yus, M. *Tetrahedron* **2011**, *67*, 3140−3149.
(15) (a) Zhao, Y. S.; Foo, S. W.; Saito, S. *Angew. Chem., Int. Ed.* **2011**, *50*, 3006−3009;(b) Martínez, R.; Ramón, D. J.; Yus, M. *Org. Biomol. Chem.* **2009**, *7*, 2176−2181.
(16) (a) Nova, A.; Balcells, D.; Schley, N. D.; Dobereiner, G. E.; Crabtree, R. H.; Eisenstein, O. *Organometallics* **2010**, *29*, 6548−6558; (b) Bosson, J.; Poater, A.; Cavallo, L.; Nolan, S. P. *J. Am. Chem. Soc.* **2010**, *132*, 13146−13149;(c) Handgraaf, J.-W.; Meijer, E. J. *J. Am. Chem. Soc.* **2007**, *129*, 3099−3103;(d) Privalov, T.; Samec, J. S. M.; Bäckvall, J.-E. *Organometallics* **2007**, *26*, 2840−2848;(e) Comas-Vives, A.; Ujaque, G.; Lledós, A. *Organometallics* **2007**, *26*, 4135−4144.
(17) Yamakawa, M.; Ito, H.; Noyori, R. *J. Am. Chem. Soc.* **2000**, *122*, 1466−1478.
(18) Zhao, G. M.; Liu, H. L.; Huang, X. R.; Zhang, D. D.; Yang, X. *RSC Adv.* **2015**, *5*, 22996−23008.
(19) Fristrup, P.; Tursky, M.; Madsen, R. *Org. Biomol. Chem.* **2012**, *10*, 2569−2577.
(20) Balcells, D.; Nova, A.; Clot, E.; Gnanamgari, D.; Crabtree, R. H.; Eisenstein, O. *Organometallics* **2008**, *27*, 2529−2535.
(21) (a) Li, H.; Lu, G.; Jiang, J.; Huang, F.; Wang, Z.-X. *Organometallics* **2011**, *30*, 2349−2363;(b) Hopmann, K. H.; Bayer, A. *Organometallics* **2011**, *30*, 2483−2497;(c) Handgraaf, J.-W.; Reek, J. N. H.; Meijer, E. J. *Organometallics* **2003**, *22*, 3150−3157.
(22) (a) Ozawa, F.; Okamoto, H.; Kawagishi, S.; Yamamoto, S.; Minami, T.; Yoshifuji, M. *J. Am. Chem. Soc.* **2002**, *124*, 10968−10969; (b) Yang, S.-C.; Hung, C.-W. *J. Org. Chem.* **1999**, *64*, 5000−5001.
(23) Martínez-Asencio, A.; Yus, M.; Ramon, D. J. *Synthesis* **2011**, *2011*, 3730−3740.
(24) Dang, T. T.; Ramalingam, B.; Shan, S. P.; Seayad, A. M. *ACS Catal.* **2013**, *3*, 2536−2540.
(25) (a) Ding, B.; Zhang, Z.; Liu, Y.; Sugiya, M.; Imamoto, T.; Zhang, W. *Org. Lett.* **2013**, *15*, 3690−3693;(b) Gowrisankar, S.; Neumann, H.; Beller, M. *Angew. Chem., Int. Ed.* **2011**, *50*, 5139−5143; (c) Gowrisankar, S.; Sergeev, A. G.; Anbarasan, P.; Spannenberg, A.; Neumann, H.; Beller, M. *J. Am. Chem. Soc.* **2010**, *132*, 11592−11598; (d) Muller, J. A.; Goller, C. P.; Sigman, M. S. *J. Am. Chem. Soc.* **2004**, *126*, 9724−9734.
(26) Frisch, M. J.; Trucks, G. W.; Schlegel, H. B.; Scuseria, G. E.; Robb, M. A.; Cheeseman, J. R.; Scalmani, G.; Barone, V.; Mennucci, B.; Petersson, G. A.; Nakatsuji, H.; Caricato, M.; Li, X.; Hratchian, H. P.; Izmaylov, A. F.; Bloino, J.; Zheng, G.; Sonnenberg, J. L.; Hada, M.; Ehara, M.; Toyota, K.; Fukuda, R.; Hasegawa, J.; Ishida, M.; Nakajima, T.; Honda, Y.; Kitao, O.; Nakai, H.; Vreven, T.; Montgomery, J. A., Jr.; Peralta, J. E.; Ogliaro, F.; Bearpark, M.; Heyd, J. J.; Brothers, E.; Kudin, K. N.; Staroverov, V. N.; Kobayashi, R.; Normand, J.; Raghavachari, K.; Rendell, A.; Burant, J. C.; Iyengar, S. S.; Tomasi, J.; Cossi, M.; Rega, N.; Millam, N. J.; Klene, M.; Knox, J. E.; Cross, J. B.; Bakken, V.; Adamo, C.; Jaramillo, J.; Gomperts, R.; Stratmann, R. E.; Yazyev, O.; Austin, A. J.; Cammi, R.; Pomelli, C.; Ochterski, J. W.; Martin, R. L.; Morokuma, K.; Zakrzewski, V. G.; Voth, G. A.; Salvador, P.; Dannenberg, J. J.; Dapprich, S.; Daniels, A. D.; Farkas, Ö; Foresman, J. B.; Ortiz, J. V.; Cioslowski, J.; Fox, D. J. *Gaussian09*, revision A.02; Gaussian, Inc.: Wallingford, CT, 2009.
(27) Becke, A. D. *J. Chem. Phys.* **1993**, *98*, 5648−5652.
(28) Lee, C.; Yang, W.; Parr, R. G. *Phys. Rev. B: Condens. Matter Mater. Phys.* **1988**, *37*, 785−789.
(29) Marenich, A. V.; Cramer, C. J.; Truhlar, D. G. J. *J. Phys. Chem. B* **2009**, *113*, 6378−6396.
(30) Krishnan, R.; Binkley, J. S.; Seeger, R.; Pople, J. A. *J. Chem. Phys.* **1980**, *72*, 650−654.
(31) Hay, P. J.; Wadt, W. R. *J. Chem. Phys.* **1985**, *82*, 299−310.
(32) Hehre, W. J.; Ditchfield, R.; Pople, J. A. *J. Chem. Phys.* **1972**, *56*, 2257−2261.
(33) (a) Fukui, K. *Acc. Chem. Res.* **1981**, *14*, 363−368;(b) Fukui, K. *J. Phys. Chem.* **1970**, *74*, 4161−4163.
(34) (a) Zhao, Y.; Truhlar, D. G. *Acc. Chem. Res.* **2008**, *41*, 157−167; (b) Zhao, Y.; Truhlar, D. G. *J. Chem. Phys.* **2006**, *125*, 194101−194118.
(35) (a) Roy, L. E.; Hay, P. J.; Martin, R. L. *J. Chem. Theory Comput.* **2008**, *4*, 1029−1031;(b) Ehlers, A. W.; Bohme, M.; Dapprich, S.; Gobbi, A.; Hollwarth, A.; Jonas, V.; Kohler, K. F.; Stegmann, R.; Veldkamp, A.; Frenking, G. *Chem. Phys. Lett.* **1993**, *208*, 111−114.
(36) Perdew, J. P.; Wang, Y. *Phys. Rev. B: Condens. Matter Mater. Phys.* **1992**, *45*, 13244−13249.
(37) Tao, J. M.; Perdew, J. P.; Staroverov, V. N.; Scuseria, G. E. *Phys. Rev. Lett.* **2003**, *91*, 146401−146404.
(38) Ernzerhof, M.; Scuseria, G. E. *J. Chem. Phys.* **1999**, *110*, 5029−5036.
(39) (a) Chai, J. D.; Head-Gordon, M. *Phys. Chem. Chem. Phys.* **2008**, *10*, 6615−6620;(b) Chai, J. D.; Head-Gordon, M. *J. Chem. Phys.* **2008**, *128*, 084106.
(40) Zhao, G. M.; Liu, H. L.; Zhang, D. D.; Huang, X. R.; Yang, X. *ACS Catal.* **2014**, *4*, 2231−2240.
(41) Hartwig, J. F. *Organotransition metal chemistry: from bonding to catalysis*; University Science: Sausalito, CA, 2010; pp 355−356.
(42) (a) Uhe, A.; Kozuch, S.; Shaik, S. *J. Comput. Chem.* **2011**, *32*, 978−985;(b) Meir, R.; Kozuch, S.; Uhe, A.; Shaik, S. *Chem. - Eur. J.* **2011**, *17*, 7623−7631.
(43) Hall, N. E.; Smith, B. J. *J. Phys. Chem. A* **1998**, *102*, 4930−4938.
(44) Li, H.; Wang, X.; Wen, M.; Wang, Z.-X. *Eur. J. Inorg. Chem.* **2012**, *31*, 5011−5020.
(45) Foster, J. P.; Weinhold, F. *J. Am. Chem. Soc.* **1980**, *102*, 7211−7218.
(46) Moncho, S.; Ujaque, G.; Lledós, A.; Espinet, P. *Chem. - Eur. J.* **2008**, *14*, 8986−8994.
(47) Bartoszewicz, A.; Gonzalez Miera, G.; Marcos, R.; Norrby, P. O.; Martín-Matute, B. *ACS Catal.* **2015**, *5*, 3704−3716.
(48) (a) Li, H.; Jiang, J.; Lu, G.; Huang, F.; Wang, Z.-X. *Organometallics* **2011**, *30*, 3131−3141;(b) Friedrich, A.; Schneider, S. *ChemCatChem* **2009**, *1*, 72−73.

DOI: 10.1021/acscatal.5b01043
ACS Catal. 2015, 5, 5728−5740

(49) Carvajal, M. A.; Kozuch, S.; Shaik, S. *Organometallics* **2009**, *28*, 3656−3665.
(50) (a) Kozuch, S.; Shaik, S. *Acc. Chem. Res.* **2011**, *44*, 101−110; (b) Kozuch, S.; Shaik, S. *J. Phys. Chem. A* **2008**, *112*, 6032−6041; (c) Kozuch, S.; Shaik, S. *J. Am. Chem. Soc.* **2006**, *128*, 3355−3365; (d) Amatore, C.; Jutand, A. *J. Organomet. Chem.* **1999**, *576*, 254−278.
(51) Boys, S. F.; Bernardi, F. *Mol. Phys.* **1970**, *19*, 553−566.
(52) Martin, R. L.; Hay, P. J.; Pratt, L. R. *J. Phys. Chem. A* **1998**, *102*, 3565−3573.

DOI: 10.1021/acscatal.5b01043
ACS Catal. 2015, 5, 5728−5740